SOLUTE NUCLEATION AND GROWTH IN SUPERCRITICAL FLUID MIXTURES

Gregory T. Smedley[1], Gerald Wilemski[2], W. Terry Rawlins[3], David B. Oakes[3],
Prakash Joshi[3]. and William W. Durgin[4]

[1] *California Institute of Technology, Pasadena, CA 91125*
[2] *Lawrence Livermore National Lab, Livermore, CA 94551*
[3] *Physical Sciences Inc., Andover, MA 01810*
[4] *Worcester Polytechnic Institute, Worcester, MA 01609*

ABSTRACT

This research effort is directed toward two primary scientific objectives: (1) to determine the gravitational effect on the measurement of nucleation and growth rates near a critical point and (2) to investigate the nucleation process in supercritical fluids to aid in the evaluation and development of existing theoretical models and practical applications. A nucleation pulse method will be employed for this investigation using a rapid expansion to a supersaturated state that is maintained for $\approx$ 1 ms followed by a rapid recompression to a less supersaturated state that effectively terminates nucleation while permitting growth to continue. Nucleation, which occurs during the initial supersaturated state, is decoupled from growth by producing rapid pressure changes. Thermodynamic analysis, condensation modeling, apparatus design, and optical diagnostic design necessary for the initiation of a theoretical and experimental investigation of naphthalene nucleation from supercritical CO_2 have been completed.

INTRODUCTION

Supercritical fluids are of considerable scientific and technological interest in the fields of chromatography, solids extraction, and particle formation due to the greatly enhanced solubility of solutes. Supercritical fluids have liquid-like densities and gas-like compressibility; therefore, the density of the fluid and the solubility of solutes within them are a strong function of the pressure. It is precisely due to this latter behavior that particle formation in rapidly expanded supercritical solutions (RESS) is a promising application for supercritical fluid technology. Careful measurements of nucleation rates are essential for understanding the fundamental aspects underlying particle formation processes and for testing nucleation rate predictions.

In this research effort, the strong dependence of the solubility on the pressure will be exploited to produce tailored nucleation pulses in an apparatus that is capable of executing rapid pressure changes on the contained mixture. The apparatus is patterned after those used in the prior research efforts of Wagner and Strey [1] and Sieber and Woermann [2]. The nucleation pulse involves a rapid expansion to a supersaturated state that is maintained for $\approx$ 1 ms followed by a rapid recompression to a lower supersaturation that permits growth to continue. The purpose of the short supersaturated state is to eliminate significant growth so that nucleation and growth are effectively decoupled. However, under some conditions the rapidity of the expected pressure changes in this apparatus is not sufficient to decouple nucleation and growth. The nucleation rates and the growth rates will be determined experimentally using a combination of Mie scattering and extinction measurements [3]. The supercritical mixture chosen for this research is naphthalene-CO_2 due to the fact that physical properties of this system have been well studied in the past, the substances are relatively benign in the quantities used here, and the critical point of CO_2 (72.9 atm and 31°C) is readily accessible in the laboratory.

The research approach employed in this study is to: (1) utilize calculated results of thermodynamic expansions and compressions to determine the volume changes that the apparatus must be capable of in

order to cover the desired (P,T) envelope and to provide thermodynamic path input for the nucleation and growth models, (2) employ nucleation and growth models to determine operating conditions that should provide particle concentrations within the detectable limits of the optical instrumentation, (3) employ Mie calculations to determine requirements and limits for the optical diagnostics, (4) conduct experiments, (5) use the experimental results and Mie calculations to determine the refractive index, the number density, the size, and the growth rates of naphthalene particles, and (6) feed this information to the nucleation and growth models to evaluate and modify the existing models.

THERMODYNAMIC ANALYSIS

Evaluation of thermodynamic paths for the apparatus has been achieved using an equation of state for CO_2 from Ref. [4]. Isentropic expansions were calculated for supercritical CO_2 starting from initial temperatures (T) of 307(7)335 K at 200 bar and initial pressures (P) of 80(20)200 bar at 335 K. These initial conditions were selected to lie on the edges of the expected (P, T) operating envelope for the apparatus. The results are shown in Figure 1, the thick curve represents the pure gas-liquid CO_2 phase boundary, the cross-hairs demark the critical point, and the thin curves (numbered 1 through 11) represent the calculated isentropic expansion paths. Note that a volume expansion factor of 1.30 was used for each curve except curves 1 and 2, which required only a factor of 1.12 and 1.20 respectively to penetrate deeply beyond the saturation curve. Up to the phase boundary, the trajectories followed by the isentropic paths lie on thermodynamically stable states for pure CO_2. Beyond the phase boundary, the expansions produce metastable states that decay via CO_2 bubble or droplet nucleation or spinodal decomposition.

This plot reveals two issues that are worth noting. First, a strong decrease in temperature is observed during the isentropic expansions that leads to an enhanced decrease in pressure. Therefore, a volume change of 30% is sufficient to span the supercritical envelope. Second, an isentropic expansion path could be chosen such that the nucleation induction occurs very near the critical point as for example, on curve 7 which starts at 160 bar and 335 K. It may be very interesting to observe the effects of near-critical point phenomena, such as large density fluctuations, on the measured nucleation rates. In more refined consideration of the thermodynamic paths, the gas-liquid phase boundary for the CO_2/naphthalene system must be considered. Since it is the intention in this research to study the nucleation of solute particles we must avoid crossing phase boundaries that will cause nucleation of CO_2 rich droplets or bubbles.

EXPANSION CHAMBER CONDENSATION MODEL

A model that simulates the nucleation and growth of solute particles in the experimental expansion chamber has been developed. This model is being used to understand how different operating conditions affect the quality of the particle size distribution. This will aid in the selection of conditions that are more favorable for the light scattering measurements needed to determine the particle concentration.

The model uses the thermodynamic equation of state for CO_2 discussed above, a nucleation rate model based on classical homogeneous nucleation with the reversible work of critical nucleus formation modified to account for the extreme nonideality of the naphthalene-CO_2 fluid mixture [5], and a particle growth model that also handles the statistical characterization of the particle size distribution. The equilibrium concentration of dissolved naphthalene is calculated using a Peng–Robinson equation of state for the mixture [6]. The isentropic expansion calculation was modified to allow the volume change of the test chamber to be parametrically specified as a function of time. At each point in the process, the nucleation rate is computed, and once a sufficiently high value is achieved, the particle growth model is used to track the sizes of all the particles formed. The particle growth rates are computed using a growth law developed by Young [7] as simplified by Peters and Paikert [8]. This growth law is quite general, covering the entire range from

free molecular to continuum behavior. Given the relatively high density of the CO_2 solvent in the region of interest, the diffusion-controlled continuum regime will be most important.

Two simulations of potential experiments are presented here to illustrate the very different types of behavior that are possible. In both cases, initially saturated mixtures are at equilibrium at the upper right end of the paths, path 6 and path 10, indicated by •'s in Figure 1. The mixtures were expanded in 3 ms to the (P,T) indicated by o's where a nucleation period was maintained for 1 ms. Finally the mixtures were compressed in 0.3 ms to the (P,T) indicated by $\triangle$'s. Both mixtures were expanded to produce similar nucleation rates ($\approx 2 \times 10^7$ s^{-1}cm^{-3}) and therefore similar particle number concentrations ($\approx 2 \times 10^4$ cm^{-3}). The behavior of the simulated particle size distributions is shown in Figure 2 at four successive times starting at the end of the nucleation period (0 ms) and ending at 10 ms. The most obvious feature of these distributions is the difference in their breadth and their height; however, the integrated particle number under each distribution is approximately constant. Due to the rapidity of particle growth under the conditions used on path 6, particles of 1 μm radius are already present at the end of the nucleation period whereas the particles created along path 10 do not grow that large in 10 ms. In both cases, the size distributions narrow at later times because growth rates are higher for smaller particles than for larger ones, but the presence of large particles during the nucleation period for path 6 eliminates the possibility of using the first Mie resonance to accurately determine the concentration of nucleated particles. The results along path 10 exhibit a much slower rate of growth and a significantly narrower size distribution. These conditions would be suitable for making measurements of the first Mie resonance to determine the particle concentration. The significant difference in growth rates is due to the reduced amount of solute present in the mixture on path 10 compared to the mixture on path 6.

APPARATUS DESIGN CONCEPT

A membrane cell, in which the lower wall is a flexible diaphragm, is the focus of the current design effort. The cell is compact, measuring 3.25″ OD × 2.0″ Tall with an internal volume of 9.3 cm^3 (1.2″ ID × 0.5″ Tall). The radius of curvature of the membrane and the ratio of the height to the diameter of the cell have been chosen to theoretically provide a maximum volume change of 50%. The actual volume change will be limited by the various sources of dead volume and by the ability to operate the membrane over its entire design range without bursting it. The pressure of the contained mixture is varied by changing the pressure on the lower side of the diaphragm using fast valves and external reservoirs. The cell should be capable of generating rapid pressure changes, with a maximum pressure of 170 atm and initial temperatures of 293 K to 358 K with the current instrumentation.

The cell is designed to allow the top part to be replaced. For example, a top that is quite tall would enable measurement of the nucleation rate at well separated points to determine gravitational effects. By maintaining the same internal volume as the original top, it would be possible to use the same membrane, valves, and reservoirs to impose the desired pressure changes.

A cross-section of the cell is shown in Figure 3 to indicate the location of the instrumentation for pressure and temperature measurement, the windows for optical access, and the inflow/outflow ports/valves for the sample mixture. A piezo-resistive pressure transducer is used to measure both the static and dynamic pressure. A thermocouple is positioned near the inner wall of the cell to measure the temperature. Multiple optical access ports are provided to enable measurements at a variety of angles. This provides some options which might be useful as cross checks or to aid in the pinpointing of the refractive index of naphthalene.

OPTICAL DIAGNOSTICS

The optical diagnostics will include simultaneous observation of the extinction at 0° and the forward scattering at 15°. These measurements permit the determination of scattering/extinction ratios as a function

of time during the growth phase of the experiment. These ratios are used to determine the particle size as a function of time, independent of the particle number density. Figure 4 shows plots of this ratio vs particle size for 15° scattering using two likely values for the refractive index of naphthalene. Once the size-vs-time dependence is known, the scattering and/or extinction signals can then be used to determine the particle number densities.

A sensitive measurement of the extinction is made by ratioing the transmitted and reference beams that result from splitting the original laser beam. The ratio removes fluctuations in the laser output, so that the measurement is affected only by slow thermal drifts in the optical train. The best sensitivity is achieved when the reference and transmitted beams have comparable intensities so the same shot noise limit can be attained in both detectors. For this condition, the measurement sensitivity is limited primarily by the dynamic range of the data acquisition system. With considerable care and a high-precision data acquisition system, extinction ratios down to perhaps 10^{-4} should be achievable. Based on Mie calculations, the ability to determine extinction ratios as low as 10^{-4} should make it possible to measure particle number densities above 3×10^4 cm^{-3} over the entire size range of interest (0.2 μm to 2 μm).

The scattered power viewed by the detector is determined by the Mie scattering calculations, the particle number density, and the geometry of the cell. To experimentally measure this scattered light over the range of particle sizes (0.2 μm to 2 μm) and number densities (300 cm^{-3} to 3×10^6 cm^{-3}), the detector must have high sensitivity to discern the lower range and must have a wide dynamic range to be able to capture the upper range. Some types of photomultiplier tubes have greater sensitivity than avalanche photodiode detectors (APD), but the APD has a greater dynamic range which makes it the detector of choice for this experiment. The expected range of the scattering signal, determined from Mie calculations of the scattered light intensity and the vendor specifications of the APD is plotted in Figure 5 for the two extremes of particle number density. Signal-to-noise estimates based on APD performance specifications and the cell geometry indicate that particle number densities of 300 cm^{-3} (4 particles/scattering volume) should be detectable over the size range of interest. Indeed, it should be possible to observe single-particle scattering over much of this range. However, to ensure favorable particle counting statistics, it is desirable to operate the experiment with particle number densities above 3×10^4 cm^{-3} where extinction measurements can be made as well (see previous paragraph).

A major concern in these measurements is the uncertainty in the refractive index of naphthalene particles at the experimental temperatures, wavelength, and pressure. A source for the refractive index of CO_2 has been located in Ref. [9]. Knowing the refractive index of CO_2 with some confidence, the refractive index n of the naphthalene particles can be determined from the scattering/extinction data through comparisons of observed and computed relative peak intensities. This is illustrated in Figure 4 where two scattering/extinction ratios are plotted, one for $n = 1.4$ and the other for $n = 1.6$; therefore, the combination of experimental measurements and Mie calculations should yield the refractive index for naphthalene under the experimental conditions.

CONCLUDING REMARKS

The chamber model enables us to explore potential experimental conditions to identify those that may result in narrow distributions of small particles at the end of the nucleation period. This model has already demonstrated the importance of avoiding particle growth rates so large that nucleation and growth cannot be decoupled even during induction times as short as 1 ms. Although the growth model should be reasonably accurate, it is worth noting that the predicted nucleation rates are notoriously inaccurate and could be off by many orders of magnitude. With inaccuracies in the prediction of nucleation rates, the resulting particle concentrations may be above or below the measurement range of the optical diagnostics. In the end, accurate empirical data from the apparatus will provide the means necessary to test and refine these models.

ACKNOWLEDGEMENTS

REFERENCES

[1] P.E. Wagner and R. Strey,"Homogeneous nucleation rates of water vapor measured in a two-piston expansion chamber", *J. Phys. Chem.* **85**(18), pp. 2694-2698, (1981).

[2] M. Sieber, and D. Woermann,"Study of non-equilibrium states of a homogeneous 2-butoxyethanol/water mixture of critical composition in the vicinity of its lower critical point using fast pressure jumps", *Ber. Bunsenges. Phys. Chem.* **95**(1), pp. 15-23, (1991).

[3] P.E. Wagner,"A constant-angle Mie scattering method (CAMS) for investigation of particle formation processes", *J. Coll. Inter. Science* **105**(2), pp. 456-467, (1985).

[4] W.C. Reynolds, *Thermodynamic Properties in SI*, (Dept. of Mechanical Engineering, Stanford, 1979).

[5] P.G. Debenedetti, "Homogeneous nucleation in supercritical fluids", *AIChE J.*, **36**, pp. 1289-1298, (1990).

[6] S.I. Sandler, *Chemical and Engineering Thermodynamics*, 2nd Ed., (Wiley, New York, 1989).

[7] J.B. Young, "The condensation and evaporation of liquid droplets at arbitrary Knudsen number in the presence of an inert gas", *Int. J. Heat Mass Transfer*, **36**, pp. 2941-2956, (1993).

[8] F. Peters and B. Paikert, "Measurement and interpretation of growth and evaporation of monodispersed droplets in a shock tube", *Int. J. Heat Mass Transfer*, **37**, pp. 293-302, (1994).

[9] J. Obriot, J. Ge, T.K. Bose and J.M. St-Arnaud, "Determination of the density from simultaneous measurements of the refractive index and the dielectric constant of gaseous CH_4, SF_6 and CO_2", *Fluid Phase Equilibria*, **86**, pp. 315-350, (1993).
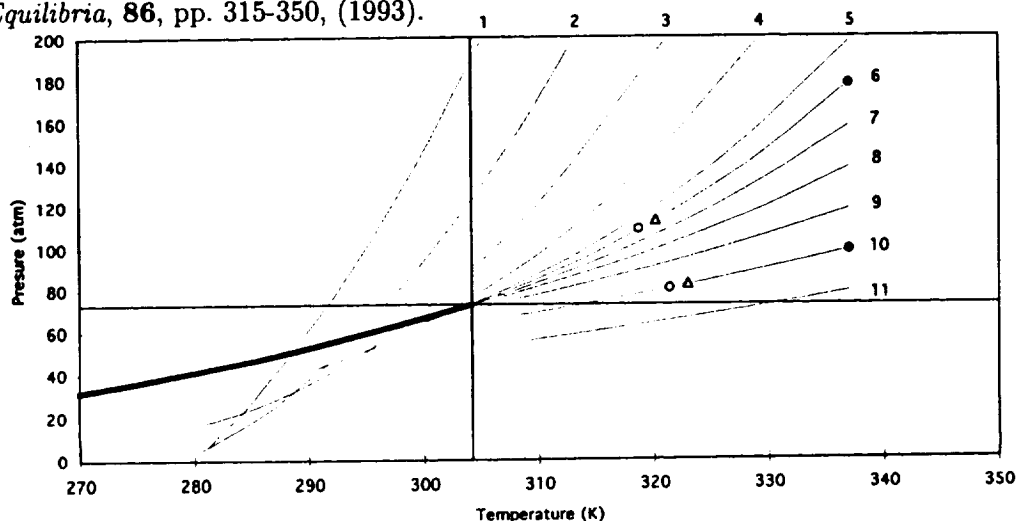

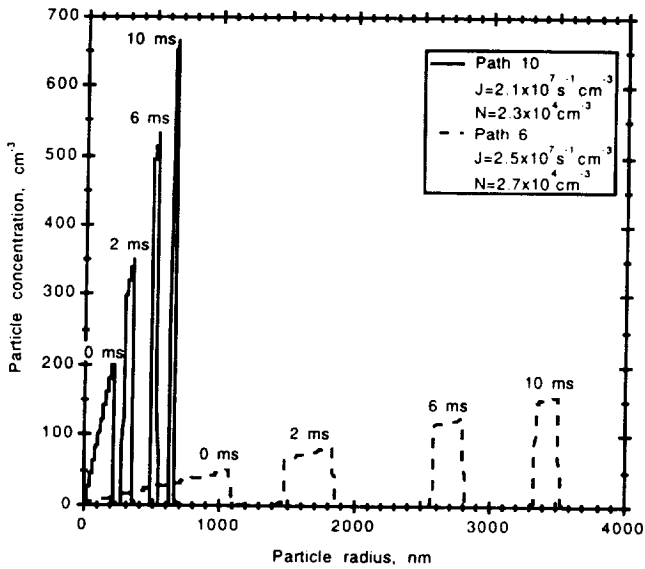Figure 1: Isentropic Expansions for pure CO_2 that span the expected experimental envelope.

Figure 2: Size distributions for the total particle density N at the indicated times measured from the end of a 1 ms nucleation period at rate J
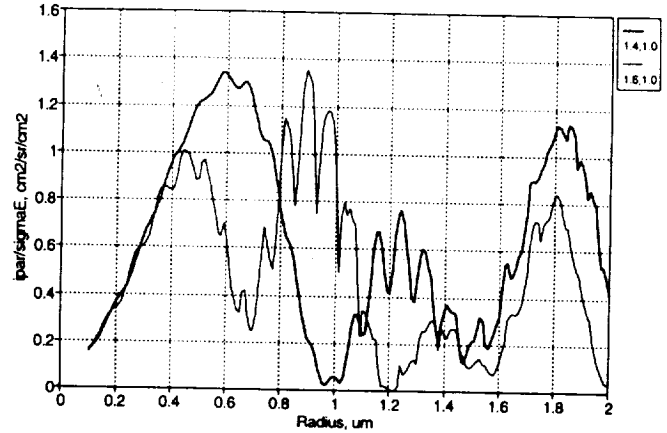

Figure 4: Scattering/Extinction ratios for two likely values of the refractive index of naphthalene $n = 1.4$ and 1.6, at 15° forward angle, CO_2 refractive index $n_m = 1.0$, and laser wavelength $\lambda = 670$ nm.
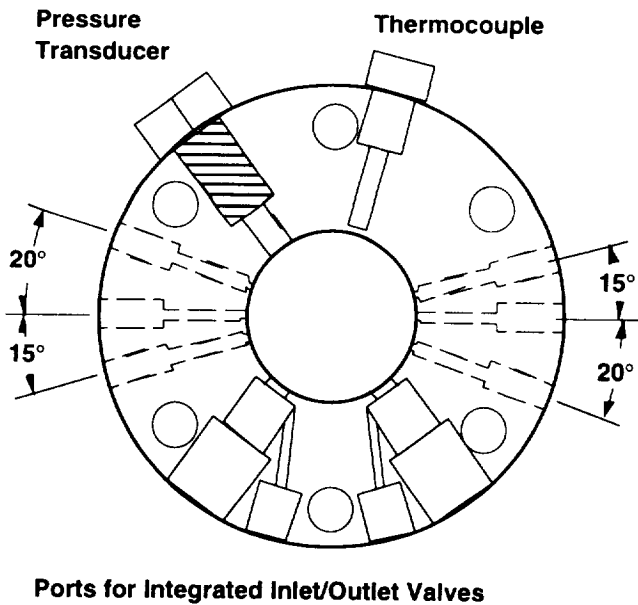

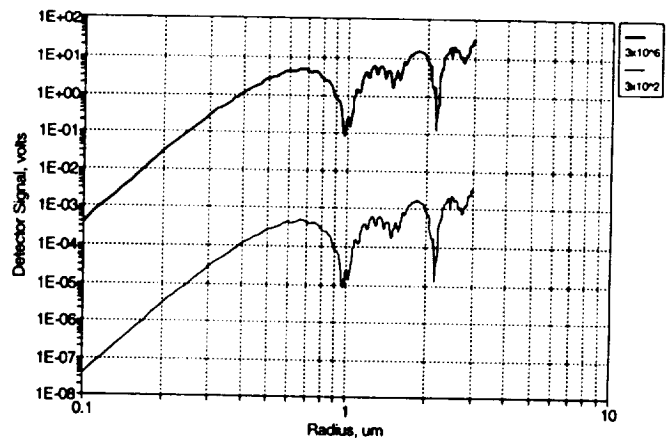Figure 3: Top view of the general layout of instrumentation and ports for the expansion chamber.

Figure 5: Calculated scattering detector signals for two extremes of the particle density (300 and 3×10^6) at 15° forward angle, $n = 1.4$, $n_m = 1.0$, and $\lambda = 670$ nm.

66